

Dynamics of Invasion Percolation

Liv Furuberg,⁽¹⁾ Jens Feder,⁽¹⁾ Amnon Aharony,^(1,2) and Torstein Jøssang⁽¹⁾

⁽¹⁾*Department of Physics, University of Oslo, Box 1048 Blindern, 0316 Oslo 3, Norway*

⁽²⁾*School of Physics and Astronomy, Beverly and Raymond Sackler Faculty of Exact Science, Tel Aviv University, Tel Aviv 69978, Israel*

(Received 30 June 1988)

Simulations of the growth of planar invasion percolation clusters exhibit novel dynamic scaling. The probability to invade a site at a distance r from a reference site at a time t after that site was invaded behaves as $N(r,t) = r^{-1}f(r^D/t)$, where D is the fractal dimension of the invaded region. The scaling function has the unusual timing behavior $f(u) \sim u^a$ ($u \ll 1$) and $\sim u^{-b}$ ($u \gg 1$), with $a \approx 1.4$, $b \approx 0.6$, and growth occurring mainly around $r \sim t^{1/D}$.

PACS numbers: 64.60.Ak, 05.40.+j, 47.55.Mh

Invasion percolation^{1,2} is a *dynamic* percolation process introduced by Wilkinson and Willemsen² motivated by the study of the displacement of one fluid by another fluid in a porous medium.^{3,4} Both standard percolation processes⁵ and invasion percolation generate self-similar *fractal*⁶ structures. A review of fractals and of experimental results⁷⁻⁹ obtained in fluid displacement processes is given in a recent book.¹⁰

Dynamics of displacement fronts is essential for understanding displacement processes in oil production, and invasion percolation is the simplest model with non-trivial front structure and dynamics.

When water is injected very slowly into a porous medium filled with oil, the capillary forces dominate the viscous forces, and the dynamics is determined by the local pore radius r . Capillary forces are strongest at the narrowest pore necks. It is consistent with both a simple theoretical model and experimental observations to represent the displacement as a series of discrete jumps in which at each time step the water displaces oil from the smallest available pore.

Wilkinson and Willemsen² simulated the model on a regular lattice. Sites and bonds represented pores and throats and were assigned random "radii." For convenience, one assumes that the easily invaded throats are invaded instantaneously, and one assigns random numbers r in the range $[0,1]$, representing the pore sizes, to the sites.

Growth sites are identified as the sites that belong to the defending fluid and are neighbors to the invading fluid. At every time step the invading fluid is advanced to the growth site that has the lowest random number r .

The invading fluid may *trap* regions of the defending fluid. As the invader advances it is possible for it to completely surround regions of the defending fluid, i.e., completely disconnect finite clusters of the defending fluid from the exit sites of the sample. This is one origin of the phenomenon of "residual oil," a great economic problem in the oil industry. Since oil is incompressible, Wilkinson and Willemsen² introduced the rule that wa-

ter cannot invade trapped regions of oil. This rule is implemented by removal of growth sites in regions completely surrounded by the invading fluid from the list of growth sites.

Figure 1 shows the results of a simulation of the invasion process. As discussed in more detail below, each color indicates sites added within a time interval $t = 2121$. The number of sites, $M(L)$, that belong to the central $L \times L$ part of an $L \times 2L$ lattice, with injection from one side, scales with the size of the lattice,²

$$M(L) = AL^D, \text{ with } D \approx 1.82. \quad (1)$$

This is consistent with the experiments of Lenormand and Zarcone⁷ of air invading slowly into a network of ducts filled with glycerol. These results should be contrasted with the ordinary percolation process for which the cluster is found by occupation of all available sites with random numbers $r \leq p$ that are connected to the seed, and p is a prechosen occupation probability. At the percolation threshold $p = p_c$, the incipient percolation cluster also obeys Eq. (1), but with the higher fractal dimensionality⁵ $D = 91/48 \approx 1.895\dots$. There are two main differences between ordinary and invasion percolation. First, invasion percolation will *always* span the region between the injection and extraction sites. There is no analog to the occupation probability p , and there are no "invader" finite clusters. Second, invasion percolation is a *dynamic* process, with a well defined sequence of invaded sites. Previous studies measured only the *static* fractal dimension D of the final aggregate. In this Letter we present the first detailed investigation of the *dynamics*.

The first hints to the nature of the dynamics came from experiments on drying⁹ and on slow fluid displacements.¹¹ In both cases, the front moved by invading local areas in *bursts*. Figure 1 shows a similar behavior: Once a new site was invaded, the front tended to stay in that vicinity. The growth within a time interval t tends to occur within a *connected* region, and the different colored regions have similar linear extensions, of order

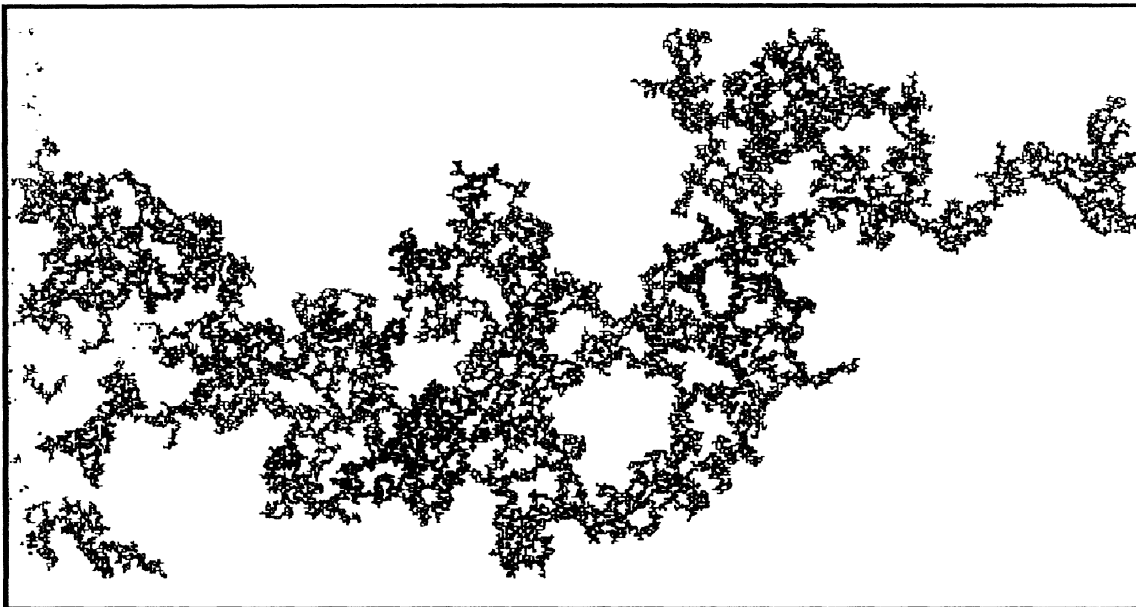


FIG. 1. Invasion percolation with trapping on a 300×600 lattice. The invader (colored) enters from sites on the left-hand edge and the defender (white) escapes through the right-hand edge. At breakthrough the invader first reaches the right-hand edge and has invaded 31 802 sites. Different colors (left to right on color scale) indicate sites added within successive time intervals $t = 2121$.

$r_t \sim t^{1/D}$. Qualitatively, this can be understood: The invading front exhausts all easily invaded pores, then by forcing the invader through a difficult pore a new region, which may have new easily invaded areas, is made available to the front. The front then moves into this area until it gets stuck again having exhausted the new easily invaded pores.

To obtain a *quantitative* measurement of these time correlations, we considered the pair correlation function $N(r, t)$, giving the probability that a site at a distance r from a reference site is invaded at a time t later than the reference site. Thus $N(r, t) dr dt$ is the conditional probability that if a site at the position r_0 was invaded at time t_0 , another site at a distance between r and $r + dr$ away from r_0 is invaded in a time interval dt around $t_0 + t$. During the simulations, the reference site is successively chosen to be the last invaded site. After some initial transient effects, the function $N(r, t)$ is found to be independent of t_0 . This is expected since the invasion process is governed by local rules, and the surroundings of every new invaded site is statistically similar to the surroundings of any other invaded site independent of how far the process has developed.

We find that the correlation function obeys the *dynamic scaling* form

$$N(r, t) = r^{-1} f(r^2/t), \quad (2)$$

with the new dynamic exponent

$$z = D. \quad (3)$$

We also find that the scaling function $f(u)$ is peaked at $u \sim 1$, and has an unusual limiting power-law behavior at both limits,

$$f(u) \sim \begin{cases} u^a, & u \ll 1, \\ u^{-b}, & u \gg 1, \end{cases} \quad \text{with } a \approx 1.4, b \approx 0.6. \quad (4)$$

This implies that the most probable growth occurs at $r_t \sim t^{1/D}$. At time t , most of the region within distance r_t has already been invaded, the rest of the region contains trapped defender fluid, and new growth there is rare. On the other hand, the probability to select a new growth site at $r \gg r_t$ decays rapidly with r .

In our simulations we used the algorithm described above on lattices of size $L \times 2L$ with L in the range 50–400. A simulation on a lattice of 300×600 sites took 30 central-processing-unit hours on an Apollo 4000 computer. We used impermeable horizontal walls, injected the invader at the left-hand side, and terminated the simulation when the invader reached the right-hand edge (see Fig. 1). The trapping rule is implemented as follows. The cluster of uninvaded sites in contact with the sink is found by the Hoshen-Kopelman¹² algorithm. If a growth site does *not* belong to this cluster, then it is trapped and removed from the list of growth sites. This global search for trapping is time consuming and is performed only when the last pore invaded is in a position that *may* trap a region of the defender. We find that the initial effects due to the line source of the invading fluid

decay rapidly and may be ignored for times that roughly correspond to the time when the invader first reaches a distance of $\frac{1}{2}L$ from the source line. Beyond that time we find that $N(r,t)$ does not depend on t_0 (that is how far from the source it is evaluated). We thus average over t_0 to obtain an estimate for $N(r,t)$.

In Fig. 2 we show the correlation function $N(r,t)$ obtained in extensive simulations. First, we note that for $t=1$ growth is most probable close to the previously invaded site, and that the growth decreases as a power law r^{-2} as r increases. For $t > 1$, we find that after a time t has passed, growth is most probable at some distance r_t away. We find that $r_t \sim t^{1/z}$ with $z \approx 1.8$. These results suggest the scaling form given in (2), which leads to the very satisfying data collapse shown in Fig. 3 with $z = 1.82$.

The straight segments in Fig. 3 give rise to the limiting behaviors in Eq. (4), implying that

$$N(r,t) \sim \begin{cases} r^{aD-1}t^{-a}, & r \ll r_t, \\ r^{-bD-1}t^b, & r \gg r_t. \end{cases} \quad (5)$$

The r^{-1} factor in the scaling expression (2) is a result of the normalization of the correlation function: Use of r^{-x} instead gives

$$1 = \int_0^\infty r^{-x} f(r^z/t) dr \\ = \frac{1}{z} t^{(1-x)/z} \int_0^\infty u^{(1-x-z)/z} f(u) du, \quad (6)$$

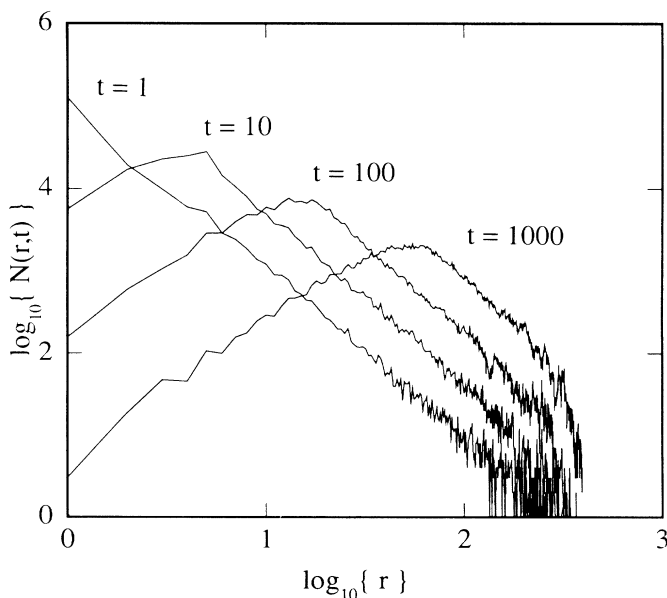


FIG. 2. The correlation function $N(r,t)$ as a function of the separation r between sites invaded with a time separation t on a log-log plot, for time separations $t=1, 10, 100$, and 1000 . The data in the figure were generated in eight simulations of the invasion percolation process on a lattice of size 300×600 . The slope of the rising part of the curves is about 1.5, and that of the falling part is about -2 .

which is independent of time only for $x=1$.

Equation (3) follows from the pair connectedness function $G(r)$, which is the probability that a site at a distance r from an occupied site is also occupied. We may express $G(r)$ in terms of $N(r,t)$ noting that (in d Euclidean dimensions) the number of sites a distance r away is $\sim r^{d-1}$

$$G(r) \sim \int_0^\infty N(r,t)/r^{d-1} dt \sim r^{z-d} \int_0^\infty u^{-2} f(u) du. \quad (7)$$

Here the integral converges. The pair connectedness function scales⁵ as $G(r) \sim r^{D-d}$ and it follows that $z=D$ as given in Eq. (3). This result can be easily intuited: t is equal to the mass of an invasion percolation cluster grown around the reference site, as represented by the different colors in Fig. 1.

Numerical simulations¹³ show that the growth sites form a fractal curve—the external perimeter.¹⁴ The number of growth sites in a circle of radius r is $M_g(r) \sim r^{D_g}$, where we find¹³ $D_g \approx 1.37$. In the simulations on strips of width L , we find that the number of growth sites becomes stationary and fluctuates around an average value $M_g(L) \sim L^{D_g}$. It is interesting to note that this new value is consistent with the fractal dimension of the external perimeter for ordinary percolation given by $D_e = \frac{4}{3}$. We expect the exponents a and b to be related to D and D_g and possibly to other exponents characterizing the growth process. However, such relations remain to be derived.

We have shown that the front of the invader in invasion percolation is characterized by a dynamic correla-

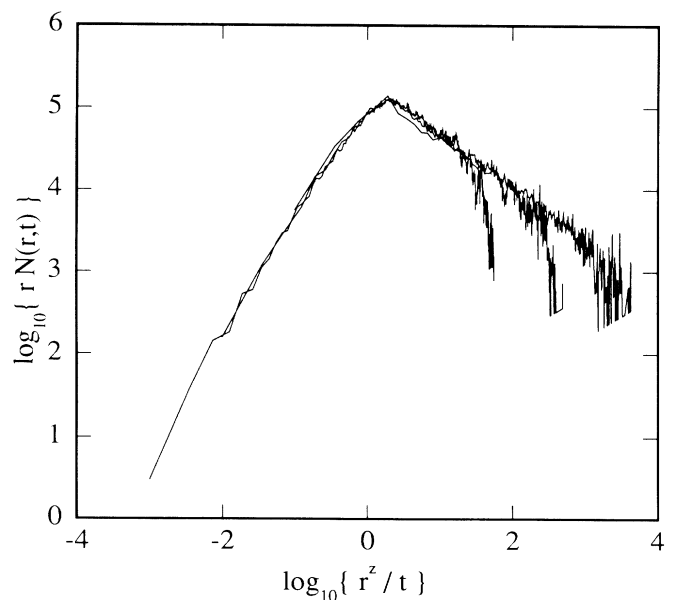


FIG. 3. Log-log plot of the scaling function $f(u) = rN(r,t)$ as a function of $u = r^z/t$ and with $z = 1.82$ obtained by reploting the results shown in Fig. 2. Finite-size effects result in a violation of the data collapse for $r \sim L$.

tion function with the rescaling form $N(r,t) = r^{-1}f(r^z/t)$, where the new dynamic exponent z is equal to the fractal dimension $D \approx 1.82$ of the invaded region. The scaling function $f(u)$ behaves as u^a for $u \ll 1$ and as u^{-b} for $u \gg 1$. Such a power-law behavior for both large and small arguments is rather surprising and remains a challenge for future theories.¹⁵

Hopefully, the present study will stimulate similar studies on other growth and fluid displacement phenomena. For example, fluid displacement at high capillary numbers leads to *viscous fingering*^{8,16} having a fractal structure^{17,18} with a fractal dimension¹⁹ $D = 1.64$. However, the scaling structure of this growth dynamics has not been investigated.

Many interesting discussions with Einar Hinrichsen and Knut Jørgen Måløy have been very helpful. The work at the University of Oslo has been supported by VISTA, a research cooperation between the Norwegian Academy of Science and Letters and Den norske stats oljeselskap a.s. (STATOIL), and by the Norwegian Council of Science and Humanities (NAVF). The work at Tel Aviv University was supported by the Israel Academy of Sciences and by the U.S.-Israel Binational Science Foundation.

¹R. Chandler, J. Koplik, K. Lerman, and J. F. Willemsen, *J. Fluid. Mech.* **119**, 249 (1982).

²D. Wilkinson and J. F. Willemsen, *J. Phys. A* **16**, 3365 (1983).

³P. G. de Gennes and E. Guyon, *J. Mec.* **17**, 403 (1978).

⁴R. Lenormand, *C. R. Acad. Sci. Paris B* **291**, 279 (1980).

⁵For reviews, see, e.g., J. W. Essam, *Rep. Prog. Phys.* **43**,

833 (1980); D. Stauffer, *Introduction to Percolation Theory* (Taylor and Francis, London, 1985); A. Aharony, in *Directions in Condensed Matter Physics*, edited by G. Grinstein and G. Mazenko (World Scientific, Singapore, 1986), p. 1.

⁶B. B. Mandelbrot, *The Fractal Geometry of Nature* (Freeman, New York, 1982).

⁷R. Lenormand and C. Zarccone, *Phys. Rev. Lett.* **54**, 2226 (1985).

⁸J. Feder, T. Jøssang, K. J. Måløy, and U. Oxaal, in *Fragmentation Form and Flow in Fractured Media*, edited by R. Engelman and Z. Jaeger, *Annals of the Israel Physical Society Vol. 8* (American Institute of Physics, New York, 1986), p. 531.

⁹T. M. Shaw, *Phys. Rev. Lett.* **59**, 1671 (1987), and in *Better Ceramics Through Chemistry II*, edited by C. J. Brinker, D. E. Clark, and D. R. Ulrich, *MRS Symposium Proceedings Vol. 73* (Materials Research Society, Pittsburgh, PA, 1986), p. 1671.

¹⁰J. Feder, *Fractals* (Plenum, New York, 1988).

¹¹K. J. Måløy, J. Feder, and T. Jøssang, unpublished observations made during the preparation of Ref. 8.

¹²J. Hoshen and R. Kopelman, *Phys. Rev. B* **14**, 3428 (1976).

¹³L. Furuberg, *Cand. Scient. thesis*, University of Oslo, 1988 (unpublished).

¹⁴T. Grossman and A. Aharony, *J. Phys. A* **19**, L745 (1986), and **20**, L1193 (1987).

¹⁵Scaling functions which vanish both at small and large arguments were seen before [M. Kolb and H. J. Herrmann, *J. Phys. A* **18**, L435 (1985)] in other problems, but they have not been analyzed for power-law behavior.

¹⁶G. M. Homsy, *Ann. Rev. Fluid. Mech.* **19**, 271 (1987).

¹⁷R. Lenormand, E. Touboul, and C. Zarccone, *J. Fluid. Mech.* **189**, 165 (1988).

¹⁸J. D. Chen and D. Wilkinson, *Phys. Rev. Lett.* **55**, 1892 (1985).

¹⁹K. J. Måløy, J. Feder, and T. Jøssang, *Phys. Rev. Lett.* **55**, 2688 (1985).

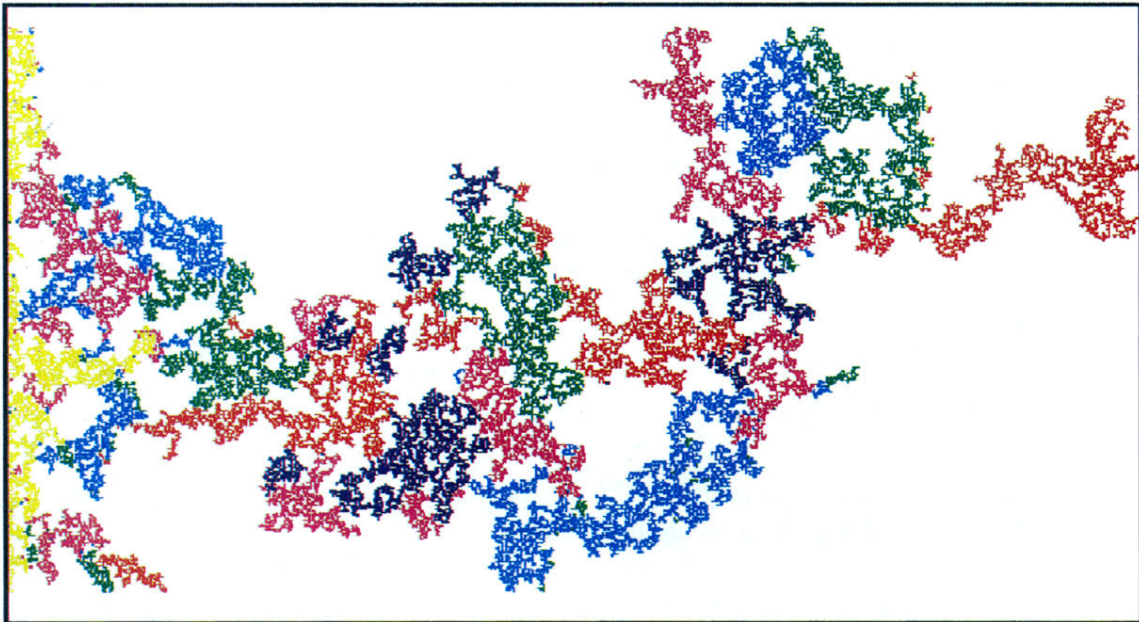


FIG. 1. Invasion percolation with trapping on a 300×600 lattice. The invader (colored) enters from sites on the left-hand edge and the defender (white) escapes through the right-hand edge. At breakthrough the invader first reaches the right-hand edge and has invaded 31 802 sites. Different colors (left to right on color scale) indicate sites added within successive time intervals $t = 2121$.